Journal of Applied Electrochemistry **33**: 85–91, 2003.

Electrolytic decomposition of amaranth dyestuff using diamond electrodes

S. HATTORI[1], M. DOI[1], E. TAKAHASHI[1], T. KUROSU[1], M. NARA[2], S. NAKAMATSU[2], Y. NISHIKI[2,*], T. FURUTA[2] and M. IIDA[3]
[1]*Department of Electronics, School of Information Technology and Electronics, Tokai University, Japan*
[2]*Development Department, Permelec Electrode Ltd, 2023-15 Endo, Fujisawa-city, Kanagawa 252-0816, Japan*
[3]*Tokai University, Junior College, Japan*
*(*author for correspondence, e-mail: nishiki@permelec.co.jp)*

Received 7 May 2002; accepted in revised form 19 September 2002

Key words: amaranth, electrolytic decomposition, decolourizing rate, diamond electrode, TOC change

Abstract

The electrolytic decomposition of an amaranth dyestuff solution using several combinations of electrodes with diamond and platinum is reported. It is observed that a portion of the amaranth is decomposed on the cathode surface while the other portion is decomposed to lower molecular weight components on the anode surface. The decolourizing rate is higher at diamond electrodes used as the anode and the cathode than with other combinations. This electrode combination also shows a rapid decrease in total organic carbon concentration. Acetic acid and oxalic acid are detected as the intermediate substances, and CO_2 gas is generated as a final product corresponding to the decrease in the oxalic acid concentration.

1. Introduction

Electrochemical treatment is a very promising method for the reduction of toxic pollutants or decolourizing by decomposing the organic substances dissolved in wastewater. It is important to select the proper electrode materials, because the electrolytic products strongly depend on those materials as well as the operating conditions [1–7].

Several researchers have been investigating electrically conductive diamond as an electrode in various electrochemical fields [8–11]. Large overvoltages were confirmed both for oxygen evolution accompanied by ozone during anodic polarization and hydrogen evolution during cathodic polarization at high current densities [12–15].

Recently, attempts have been made to fabricate new types of diamond electrodes [16–21]. Other papers deal with the current potential behaviour of typical redox couples, including oxygen reduction [22, 23].

Diamond electrodes may be used in various industrial applications, such as electrochemical synthesis and effluent water treatment, wherein water decomposition should be avoided in order to obtain a high current efficiency for the target reaction [24–27]. It has been reported that the diamond electrode has a novel ability to destroy many kinds of organic substances [28, 29].

This paper deals with the electrolytic decomposition of amaranth dyestuff solution using several types of cells composed of diamond or other electrode materials, focusing on not only decolourizing and TOC reduction rate but also on the intermediate and final products to clarify the decomposition mechanism.

2. Experimental details

Polycrystalline boron-doped diamond films were grown on a 0.007 Ω cm *p*-type silicon wafer by the hot filament-assisted chemical vapour deposition (HF-CVD) method. The Si substrates were scratched with diamond powder to enhance the diamond nucleation. The applied reactant gas was ethanol vapour containing a small amount of boron oxide, mixed with hydrogen gas. The doping level of boron in the diamond layer, expressed as the B/C ratio, ranged from 1000 to 10 000 ppm. It had been previously revealed from secondary ion microspectroscopy (SIMS) analysis that the B/C ratio was very similar to that of the original source solution. The value of the carbon and hydrogen ratio (C/H) was adjusted to 0.08. The temperatures of the filament and the substrate were controlled at about 2300 and 900 °C, respectively. The thickness of the film was about 5 μm, after keeping the substrate for 10 h in the deposition chamber.

Doped diamond electrodes were also fabricated by microwave plasma-assisted chemical vapour deposition (MW-CVD, Denki Kogyo Co., JP). The doping level of boron in the diamond layer was roughly 1500 ppm. The

films were deposited at about 900 °C. The thickness of the film was about 3 μm (12 h for deposition).

Scanning electron microscopy (SEM) images and the Raman spectra of these films showed the presence of a typical CVD diamond layer.

Three types of cell were used for the macroelectrolysis. A beaker cell containing 10 g l^{-1} of sodium sulfate (100 ml volume) was used to measure the depolarization and decomposition behaviour, wherein electrodes of 1 cm^2 area were placed at a 1 cm interelectrode gap.

A cell with a neutral separator (Poreflon, Sumitomo Electric Ind., JP) was used for evaluating the different products generated on the anode or on the cathode. For compensation of the large solution *IR*-drop of the solution due to a large electrode gap (10 cm in distance between electrodes of 1 cm^2 area), 50 g l^{-1} of sodium sulfate solution (50 ml volume) was used as the electrolyte. A platinum plate of 0.5 mm thickness (Tanaka Kikinzoku, KK, JP), a commercially available titanium plate of 1 mm thickness and a glassy carbon plate of 3 mm thickness (GC-2000, Tokai Carbon, JP) were used as comparative electrode materials.

Another cell with an ionic exchange membrane (Nafion® 117, I. E. Du Pont De Nemours, USA) was operated with no supporting electrolyte to confirm the effect of the electrolyte. A large hole of 5 mm diameter penetrated through the membrane at the bottom part in order not to separate the anolyte from the catholyte. The electrodes made of 1500 ppm B-doped MW-CVD diamond-coated on silicon segmental plates (8 cm^2 as a projected area) were connected to the membrane for electrolysing in 180 ml of pure water. Platinum electroplated titanium mesh of 0.5 mm thickness (Tanaka Kikinzoku KK, JP) was used as a comparative electrode material. The macro electrolysis in these cells was conducted at 0.01–0.2 A cm^{-2} with 0.1 g l^{-1} of amaranth at 35 °C.

The electrolysis for each condition was conducted within a period of 180 min unless otherwise noted. The electrolysis amount was expressed using QV^{-1} (Ah l^{-1}), where Q is the electrical charge (Ah) divided by the cell volume, V (l).

The change in the absorption spectra of amaranth during electrolysis was measured using an UV-250 Spectrometer (Shimadzu Corporation, JP). The ozone concentration was quantitatively confirmed by iodometry. The concentration of hydrogen peroxide was measured by the spectrometer after mixing $TiSO_4$ solution as a coloring indicator. COD_{Mn} (Chemical Oxygen Demand) titrated with $KMnO_4$ solution and TOC (Total Organic Carbon) using TOC 5000A (Shimadzu Corporation, JP) as well as the absorption spectra were measured to estimate the decomposition rate and substances. The CO_2 content was measured by a gas chromatograph (G-5000, Hitachi, JP). A high performance liquid chromatograph (HPLC) (SD-8023, Tosoh, JP) was used for identifying the intermediate organic substances at a rate of 1 ml min^{-1} for 20 mM KH_2PO_4 as the carrier solution and detected using a 216 nm light wavelength. Peroxodisulfate ion produced on the anodes was measured by HPLC and titrated with $KMnO_4$ solution.

3. Results and discussion

3.1. *Decolourizing ability*

The chemical structure and absorption spectrum of amaranth are shown in Figure 1. The peak in the spectra at around 520 nm corresponds to the representative colour of amaranth (—N=N— double bond). The decolourizing rate obtained in the beaker cell significantly depended on the anode materials, and the diamond anode showed a better performance than platinum. Moreover, the diamond electrode combination (diamond as both anode and cathode) was found to be most suitable for the decomposition, as shown in Figure 2 curve (a). The decolourizing rate also strongly depended on the cathode materials, and the diamond cathode showed better performance than the other electrodes, as shown in Figure 3. The remaining percent of the amaranth concentration after 60 min electrolysis at 0.2 A cm^{-2} was 20% for the titanium cathode, but it was still over 60% for both the platinum and GC anodes.

Considering the decomposition mechanism, the anolyte and the catholyte were separately analysed using the neutral separator cell. All the peaks in the anolytes disappeared for the diamond electrodes but remained for the platinum electrodes, as shown in Figure 4. A rapid decrease in the u.v. peaks at a wavelength smaller than 400 nm, which corresponded to the lower molecular weight components, suggested that the diamond anode could decompose the aromatic ring structure more easily than platinum.

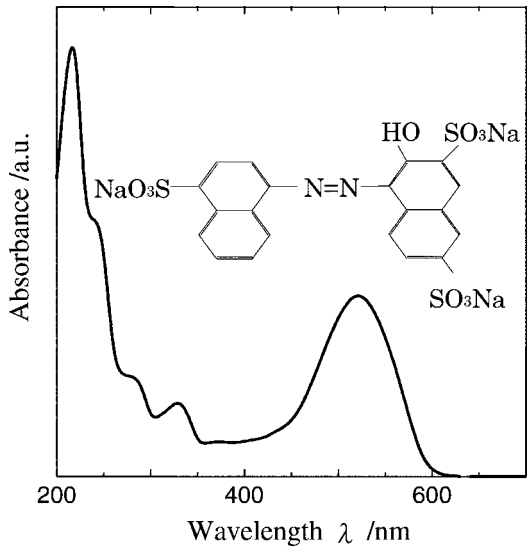

Fig. 1. Structure and absorption spectrum of amaranth.

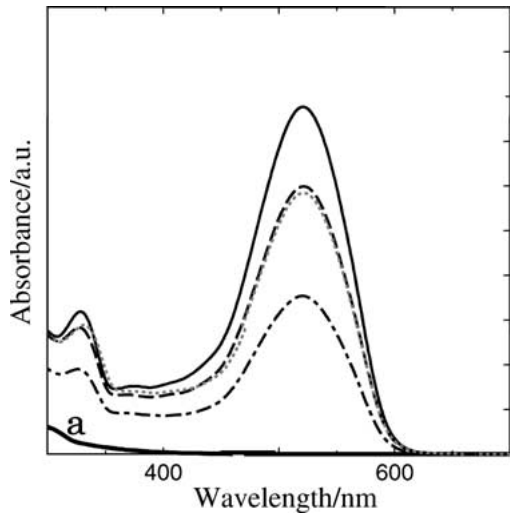

Fig. 2. Comparison of absorption spectra obtained after electrolysis with various electrode combinations using 10 000 ppm B-doped anodes, 1000 ppm B-doped cathodes and platinum electrodes, wherein curve (a) corresponds to that of the diamond electrode combination. Conditions: c.d. 0.2 A cm^{-2}; temp. 35 °C; operating time 60 min. Anode|cathode: (—) diamond|diamond; (· · · ·) Pt|Pt; (–·–) diamond|Pt; (– – –) Pt|diamond; (—) initial.

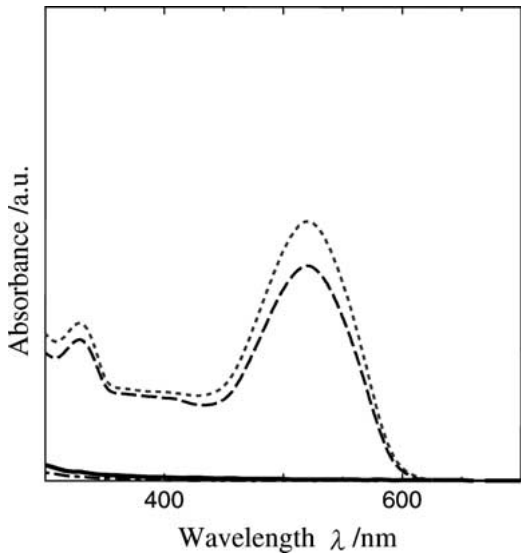

Fig. 4. Change in absorption spectra in the anolyte using the separator cell with platinum and the same diamond electrodes described in Figure 2. Conditions: c.d. 0.2 A cm^{-2}; operating time 60 min. Anode|cathode: (—) diamond|diamond; (· · ·) Pt|Pt; (–·–) diamond|Pt; (– – –) Pt|diamond.

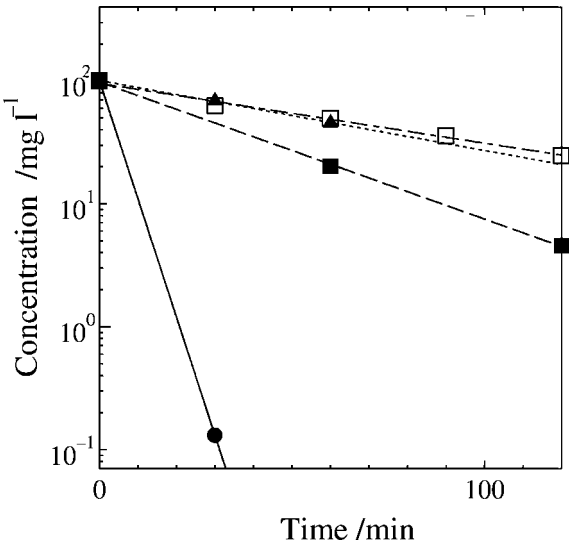

Fig. 3. Time course of amaranth concentration calculated from the absorption peak, obtained from various cathode materials using the same diamond electrodes described in Figure 2. Current density 0.2 A cm^{-2}. Cathode: (□) GC, (▲) Pt, (■) Ti and (●) diamond. Anode: diamond.

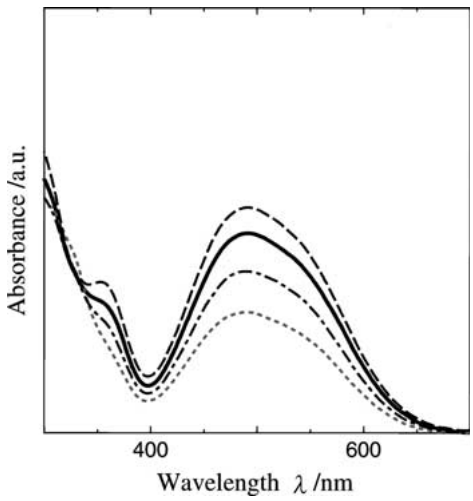

Fig. 5. Change in absorption spectra in the catholyte using the separator cell with platinum and the same diamond electrodes described in Figure 2. Conditions and legend as for Figure 4.

On the other hand, it was found in the catholytes that the decolourizing rate obtained with the platinum cathode was larger than that with diamond, as shown in Figure 5. Because the peak at around 500 nm clearly decreased, the azo-bond was also decomposed at both cathodes.

This result seemed to contradict the result obtained from the cell with no separator. The result from the separator cell seems reasonable because the catalytic activity of the platinum cathode is greater than that of the diamond cathode in relation to the reduction of the azo-bond. It could be partially understood by the fact the decolourizing rate for the platinum cathode in the beaker cell was lowered due to the presence of dissolved oxygen generated from the anode, which could be easily reduced to water on the platinum prior to the organic substances.

As the current density increased, the decolourizing rate constant estimated from the spectra data increased, as compared in Figure 6 for the diamond electrodes.

3.2. *Effect of byproducts*

To evaluate the indirect decomposition with byproducts, such as ozone, hydrogen peroxide and peroxodisulfate

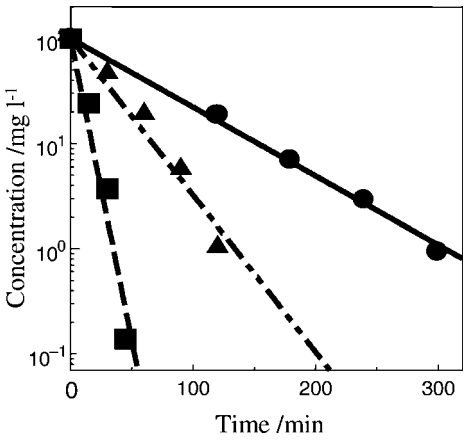

Fig. 6. Time course of amaranth concentration estimated from the absorption peak at 520 nm using the same diamond electrodes described in Figure 2. Current density: (●) 0.1, (▲) 0.05 and (■) 0.2 A cm^{-2}.

ion ($S_2O_8^{2-}$), each chemical was separately added to the amaranth solution.

It has been confirmed that ozone could be generated at the diamond anode [13]. The feed rate and concentration of ozone gas from an electrolytic ozone generator was controlled at the same value as that of the membrane cell with the 10 000 ppm B-doped diamond anode. The decolourizing rate was one tenth that of the direct electrolysis, suggesting that the main decomposition could proceed via direct oxidation on the anode.

The decolourizing behavior was also examined in pure water using a membrane cell. It was found that almost the same decolourizing rate was obtained as in the beaker cell with the Na_2SO_4 solutions. This result suggests that the effect of the peroxodisulfate ion on the decomposition of organic was negligible.

Hydrogen peroxide had no significant ability to decompose amaranth when added alone to the solution. However, the combined effect of ozone and hydrogen peroxide to produce active OH radicals must be taken into consideration. It had been revealed that a high concentration of hydrogen peroxide is obtained, as well as ozone, when using the diamond anode, resulting in a high concentration of the radicals [30].

3.3. *Analysis of decomposition products in solution*

Figure 7 shows the variations in several peaks obtained from the electrolysis at a current density of 0.2 A cm^{-2}, using the cell with the neutral separator to separately analyse the anolytes and catholytes. It was found that the peak corresponded to acetic acid (detected at 3.4 min by HPLC measurement) first increased, then disappeared with electrolysis time. The peaks at 2.54 and 4.85 min are assumed to correspond to formic acid and maleic acid, respectively. The peak corresponding to 1-aminonaphthalene-4-sulfonate ($t = 6.6$ min) or another part of the amaranth was detected at 7.5 min, suggesting that the azo-bond was reduced to generate two substances with aromatic rings. This peak was mainly observed in the solution near the cathode.

A large peak at 2.0 min that might correspond to oxalic acid or formic acid was observed in the solutions near both the anode and the cathode. However, not only peroxodisulfate ion but also hydrogen peroxide showed a peak near 2.0 min. For the purpose of identifying the peak, additional tests were conducted as follows. The peak area at 2.0 min in Figure 7 increased with increase in Na_2SO_4 concentration. As the Na_2SO_4 concentration increased, the current efficiency of $S_2O_8^{2-}$ increased and attained over 40% (9 g l^{-1}) at 250 g l^{-1} at 0.5 A cm^{-2}, though it was below the detection level (200 mg l^{-1}) when using the platinum anode. This result was in accordance with the data reported elsewhere [26].

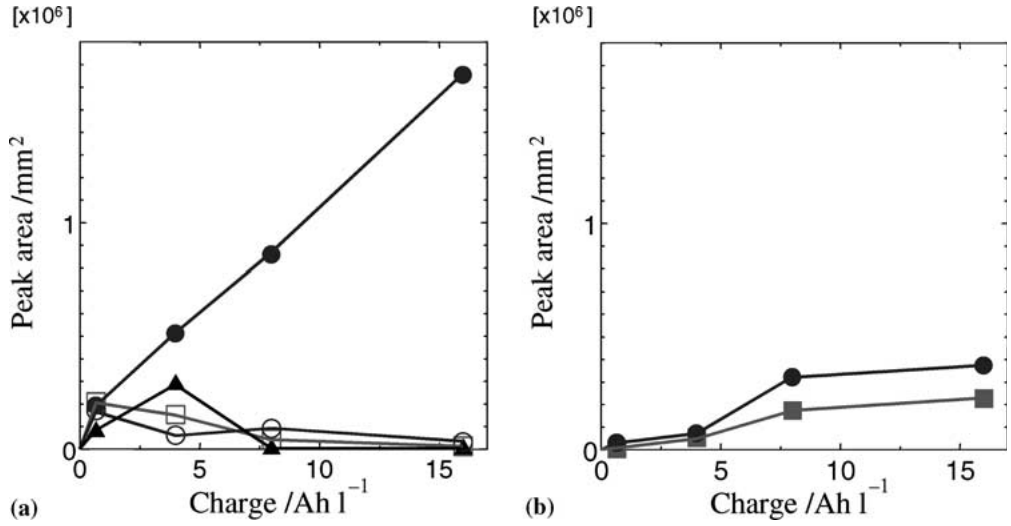

Fig. 7. Change in the HPLC peak area for the (a) anolyte and (b) catholyte corresponding to intermediates with electrical charge using the separator cell and the same diamond electrodes described in Figure 2. Retention time (a): (●) 2.00 (▲) 2.54, (○) 3.40 and (□) 4.85 min; retention time (b): (●) 2.00 and (■) 7.50 min.

To clarify the peak component, a membrane cell was operated in pure water in the absence of Na_2SO_4 to avoid the effect of its oxidized species. In the case of platinum electrodes as anode and cathode, the peak continued to increase during the measuring time as shown in Figure 8(b). For the diamond electrodes, as shown in Figure 8(a), the peaks at both 2.0 and 3.4 min (acetic acid) decreased after an initial burst in a way similar to that in the beaker cell, which showed that the peak does not correspond to the peroxodisulfate ion.

To eliminate the effect of hydrogen peroxide on the quantitative detection of oxalic acid, the amount of H_2O_2 was subtracted from the peak count. The concentration of hydrogen peroxide within the electrolysis time in pure water ranged from 16 to 27 mg l^{-1}. It was revealed that the main portion at 2.0 min belongs to oxalic acid because the peak change corresponding to the hydrogen peroxide was almost negligible.

In addition to the above analysis, oxalic acid was detected as a yellow-coloured precipitate generated in the solution when adding $FeSO_4$ as an indicator. The above results revealed that the peak at 2.0 min mainly corresponds to oxalic acid.

Figure 9 shows the change in oxalic acid concentration at the platinum and diamond electrodes. Oxalic acid was present at 40 mg l^{-1} at a maximum, compared with the platinum electrode that showed 60 mg l^{-1} at 27 Ah l^{-1} and continued to increase with time.

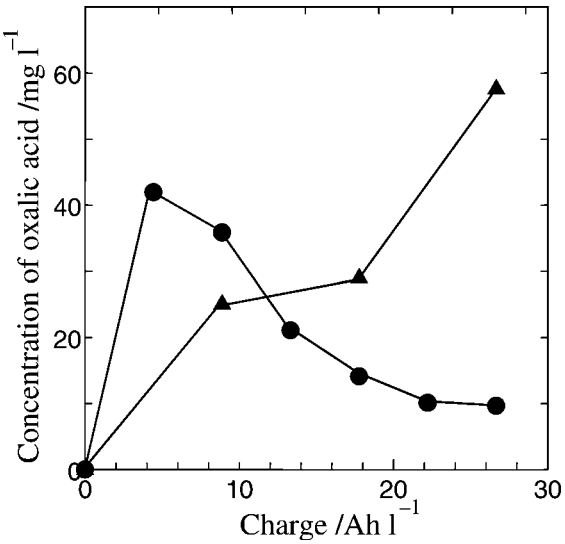

Fig. 9. Time course of oxalic acid concentration estimated from the HPLC peak area using the same diamond electrodes described in Figure 8. Anode|cathode: (●) diamond|diamond; (▲) Pt|Pt.

3.4. *TOC and COD measurements*

The variations in the TOC and COD were compared as a measure of the ability of the electrodes to decompose both the starting organic material and the intermediates using the membrane cell. On the one hand, the results shown in Figure 10, which were obtained in the membrane cell at a current density of 0.2 A cm^{-2}, suggested that the TOC was rapidly reduced as the electrolysis continued at the diamond electrode combination (remaining percentage: 6% at 27 Ah l^{-1}). On the other hand, the TOC remained almost at the same value for the platinum electrode combination (remaining percentage: 90% at 27 Ah l^{-1}).

The TOC corresponding to the concentration of oxalic acid after several hours of electrolysis (>15 Ah l^{-1}), as shown in Figure 11, suggested that most of the organic carbon actually exists as oxalic acid.

The COD removal percent after 60 min operation for the diamond anode was 69%, which was larger than that for the platinum anode by 39% and showed almost the same ability as a tin dioxide anode but better than that of a lead dioxide anode [31]. In the test of the cathode material using a diamond anode, the diamond

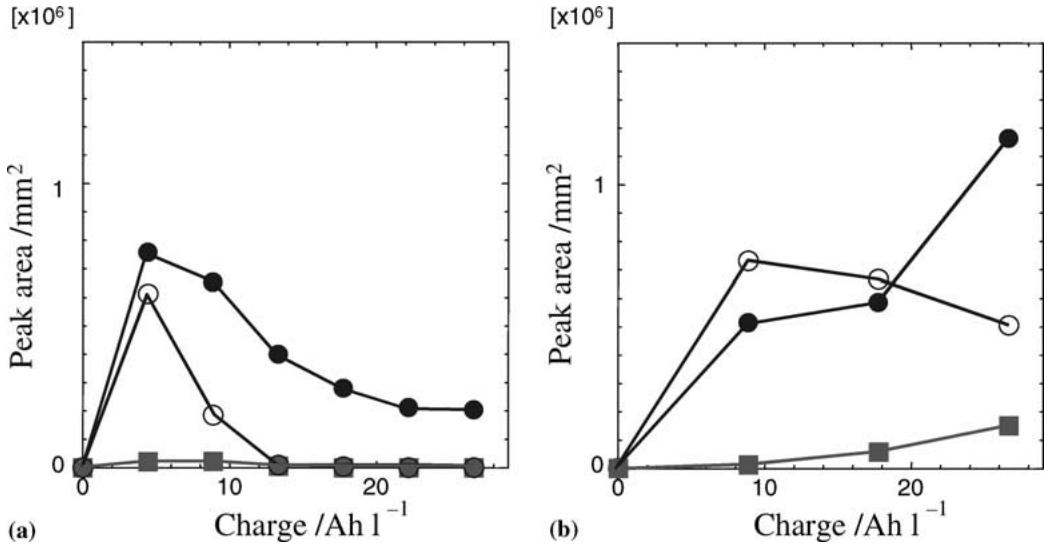

Fig. 8. Change in the HPLC peak area in the membrane cell corresponding to intermediates with electrolysis time for (a) 1500 ppm B-doped diamond electrodes and (b) platinum electrodes. Retention time (a) and (b): (●) 2.00, (○) 3.40 and (■) 7.50 min.

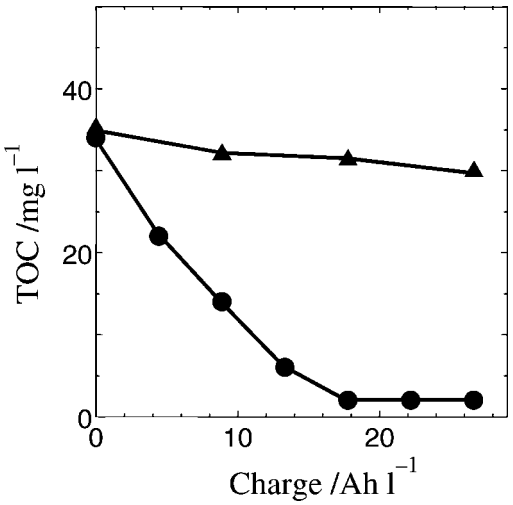

Fig. 10. Variation in remaining TOC concentration with electrical charge using the same diamond electrodes described in Figure 8. Anode|cathode: (●) diamond|diamond; (▲) Pt|Pt.

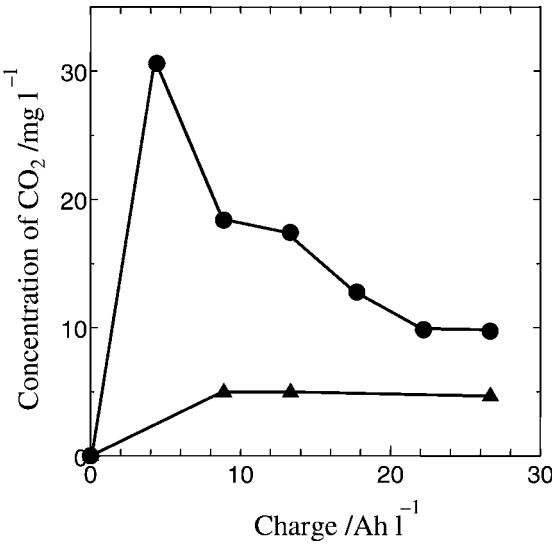

Fig. 12. Time course of CO_2 concentration in the effluent anodic gas using the same diamond electrodes described in Figure 8. Anode|cathode: (●) diamond|diamond; (▲) Pt/Pt.

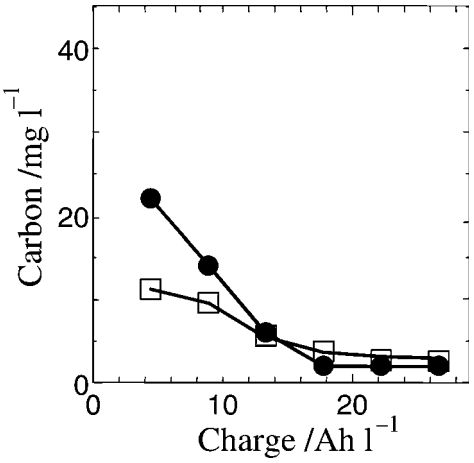

Fig. 11. Time course of carbon amounts calculated from the TOC (●) and oxalic acid (□) concentration using the same diamond electrodes described in Figure 8.

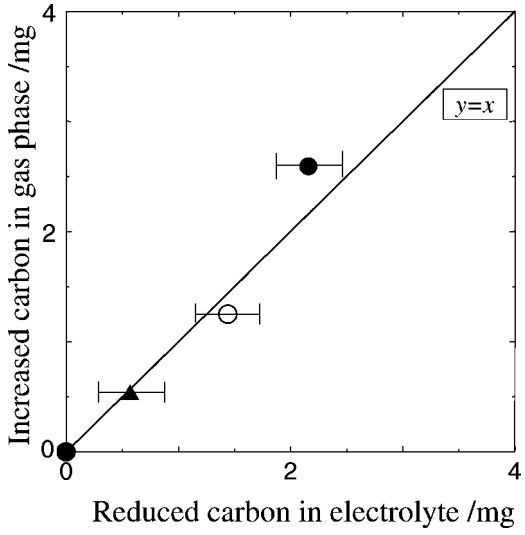

Fig. 13. Relation between carbon amounts in the generated gas (y) and the reduced TOC value in the electrolyte (x) using the same diamond electrodes described in Figure 8. Anode|cathode: (●) diamond|diamond (0–0.1 Ah); (○) diamond|diamond (0.1–0.2 Ah); (▲) Pt|Pt (0.–0.2 Ah).

cathode was superior to any other cathode and the COD became less than 1 mg l^{-1} after 90 min.

3.5. *Analysis of generated gas*

It was expected that oxalic acid would be finally oxidized to CO_2 and released from the liquid phase when diamond electrodes were used. The CO_2 concentration included in the effluent gas from the anode chamber was also measured using the membrane cell. The gas was collected for 1 h as shown in Figure 12. CO_2 gas was observed to be produced and no hydrocarbon gas was detected in the cathode gas. The reduced amount of the carbon atom (total carbon) in the solution showed good correspondence with the increased amount of that in the gas phase, as shown in Figure 13. There was a linear relation between them. The recovery percent of CO_2, which was supposed to be the final product, was about 80% at 180 min.

4. Conclusions

It was revealed that the diamond-diamond electrode combination shows better performance than other electrode combinations, such as diamond–platinum and platinum–platinum, for the decomposition of amaranth dyestuff. Based on the above analysis of the intermediate and final products of the electrolytic decomposition of amaranth using diamond electrodes, the decomposition steps were proposed as follows:

(a) Some part of the amaranth is decomposed to 1-aminonaphthalene-4-sulfonate on the cathode surface due to hydrogenation of the azo-group [32].

(b) Amaranth or hydrogenated substances are easily decomposed to lower molecular weight components on the anode, suggesting that the diamond anode could destroy the aromatic ring structure. As intermediate substances, acetic acid, maleic acid and oxalic acid were detected.
(c) Lower molecular weight substances are finally decomposed to CO_2 gas on the anode surface. No hydrocarbon was detected in the effluent gas.

The diamond electrode could decompose the organic substances not only directly but also indirectly by reacting with the produced active species, such as ozone and hydrogen peroxide, which may react with each other to generate radicals [33]. These active species are able to react with the organic substances present in the bulk solution.

An interesting result was obtained when diamond electrodes were used as both the anode and cathode in the cell with no separator. The decomposition rate was greater than that with the other combinations of electrodes, suggesting a combined mechanism between the electrodes. This suggests that a cell with no separator will give good results for decomposing organic substances, though this may depend on the kinds of effluent. It is also notable that a membrane cell composed of diamond electrodes is very applicable for an effluent that is not sufficiently conductive.

Acknowledgements

The authors wish to express their appreciation for the fruitful suggestions by Dr H. Kimura and their gratitude to Mr K. Ando, Mr H. Tachibana, and Ms R. Arai for helping with this study. They also wish to express their appreciation to Mr S. Yokoyama for permission to publish this paper.

References

1. G. Foti, D. Gandini, Ch. Comninellis, A. Perret and W. Haenni, *Electrochem. Solid State Lett.* **2** (1999) 228.
2. Gallegos and D. Pletcher, *Electrochim. Acta* **44** (1999) 2483.
3. D. Johnson, J. Feng and J. Houk, *Electrochim. Acta* **46** (2000) 323.
4. S. Stucki, R. Kotz, B. Carccer and W. Suter, *J. Appl. Electrochem.* **21** (1991) 909.
5. K. Kim, M. Kuppuswamy and R.F. Savinell, *J. Appl. Electrochem.* **30** (2000) 543.
6. G. Saracco, L. Solarino, R. Aigotti, V. Specchia and M. Maja, *Electrochim. Acta* **46** (2000) 373.
7. R. Amadelli, A. Battisti, D. Girenko, S. Kovalyov and A. Velichenko, *Electrochim. Acta* **46** (2000) 341.
8. Y.V. Pleskov, A.Y. Sakharova, M.D. Krotova, L.L. Bouilov and B.V. Spitsyn, *J. Electroanal. Chem.* **228** (1987) 19.
9. R. Tenne, K. Patel, K. Hashimoto and A. Fujishima, *J. Electroanal. Chem.* **347** (1993) 409.
10. G.M. Swain and R. Ramesham, *Anal. Chem.* **65** (1993) 345.
11. G.M. Swain, *J. Electrochem. Soc.* **141** (1994) 3382.
12. R. DeClements, B.L. Hirsche, M.C. Granger, J. Xu and G.M. Swain, *J. Electrochem. Soc.* **14** (1996) L150.
13. N. Katsuki, E. Takahashi, M. Toyoda, T. Kurosu, M. Iida, S. Wakita, Y. Nishiki and T. Shimamune, *J. Electrochem. Soc.* **145** (1998) 2358.
14. N. Katsuki, S. Wakita, Y. Nishiki, T. Shimamune, Y. Akiba and M. Iida, *Jpn. J. Appl. Phys.* **36** (1997) L260.
15. H.B. Martin, A. Argoitia, U. Landau, A.B. Anderson and J. Angus, *J. Electrochem. Soc.* **143** (1996) L133.
16. M. Granger and G. Swain, *J. Electrochem. Soc.* **146** (1999) 4551.
17. F. Bouamrane, A. Tadjeddine, R. Tenne, J.E. Butler, R. Kalish and Levy-Clement, *J. Phys. Chem. B* **102** (1998) 134.
18. Q. Chen, D. Gruen, A. Kraus and T. Corrigan, *J. Electrochem. Soc.* **148** (2001) E44.
19. B. Sarada, T. Rao, D. Tryk and A. Fijishima, *J. Electrochem. Soc.* **146** (1999) 1469.
20. T. Kuo, R. McCreery and G. Swain, *Electrochem. Solid-State Lett.* **2** (1999) 288.
21. N. Vinokur, B. Miller, Y. Avyigal and R. Kalish, *J. Electrochem. Soc.* **143** (1996) L238.
22. T. Yano, D. Tryk, K. Hashimoto and A. Fijishima, *J. Electrochem. Soc.* **145** (1998) 1870.
23. T. Yano, E. Popa, D. Tryk, K. Hashimoto and A. Fijishima, *J. Electrochem. Soc.* **146** (1999) 1081.
24. M. Panizza, I. Duo, P. Michaud, G. Cerisola and Ch. Comninellis, *Electrochem. Solid-State Lett.* **3** (2000) 550.
25. F. Okino, H. Shibata, S. Kawasaki, H. Touhara, K. Momota, M. Gamo, I. Sakaguchi and T. Ando, *Electrochem. Solid-State Lett.* **2** (1999) 382.
26. P. Michaud, E. Mahe, A. Perret, W. Haenni and Ch. Comninellis, *Electrochem. Solid-State Lett.* **3** (2000) 77.
27. S. Ferro, A. Battisti, I. Duo, Ch. Comninellis, W. Haenni and A. Perret, *J. Electrochem. Soc.* **147** (2000) 2614.
28. M. Fryda, D. Herrmann, L. Schafer, C. Klages, A. Perret, W. Haenni, Ch. Comninellis and D. Gandini, *New Diamond and Frontier Carbon Tech.* **9** (1999) 229.
29. D. Gandini, E. Mahe, P. Michaud, W. Haenni, A. Perret and Ch. Comninellis, *J. App. Electrochem.* **30** (2000) 1345.
30. E. Takahashi, T. Kurosu, K. Suga, Y. Nishiki, S. Wakita, M. Tanaka and S. Nakamatsu, *Electrochem.* (*Denki Kagaku*), in preparation.
31. Y. Nakajima, M. Sekimoto, K. Hirao, T, Shimamune and Y. Matsuda, *Electrochem.* (*Denki Kagaku*) **62** (1994) 1086.
32. T.M. Florence, *Electroanal. Chem. Int. Elec.* **52** (1974) 115.
33. K. Suga, Y. Nishiki, M. Tanaka and S. Nakamatsu, *Electrochem.* (*Denki Kagaku*) **66** (1998) 856.